1,25-Dihydroxyvitamin D_3 enhances glucose-stimulated insulin secretion in mouse and human islets: a role for transcriptional regulation of voltage-gated calcium channels by the vitamin D receptor.

Running title: VDR regulates VGCC to enhance insulin secretion.

Lilja Kjalarsdottir[1,8], Sarah A. Tersey[2,3], Mridula Vishwanath[4], Jen-Chieh Chuang[1], Bruce A. Posner[4], Raghavendra G. Mirmira[2,5,6], and Joyce J. Repa[1,7,8]

Departments of [1]Physiology, [4]Biochemistry and [7]Internal Medicine, University of Texas Southwestern Medical Center, Dallas, TX 75390
Departments of [2]Pediatrics, [5]Medicine, [6]Cellular and Integrative Physiology and [3]Center for Diabetes and Metabolic Diseases, Indiana University School of Medicine, Indianapolis, IN 46202

[8]**Corresponding Author:**

Joyce J. Repa, Ph.D.
Departments of Physiology and Internal Medicine
University of Texas Southwestern Medical Center
5323 Harry Hines Blvd.
Dallas, TX 75390-9077
Phone: (1)-214-648-9431
Fax: (1)-214-648-5612
Email: joyce.repa@utsouthwestern.edu

Number of figures: 7 (2 requiring color)
Supplementary materials: 2 Tables, 1 Figure

This is the author's manuscript of the article published in final edited form as:

Kjalarsdottir, L., Tersey, S. A., Vishwanath, M., Chuang, J.-C., Posner, B. A., Mirmira, R. G., & Repa, J. J. (2018). 1,25-Dihydroxyvitamin D3 enhances glucose-stimulated insulin secretion in mouse and human islets: a role for transcriptional regulation of voltage-gated calcium channels by the vitamin D receptor. The Journal of Steroid Biochemistry and Molecular Biology. https://doi.org/10.1016/j.jsbmb.2018.07.004

Graphical Abstract

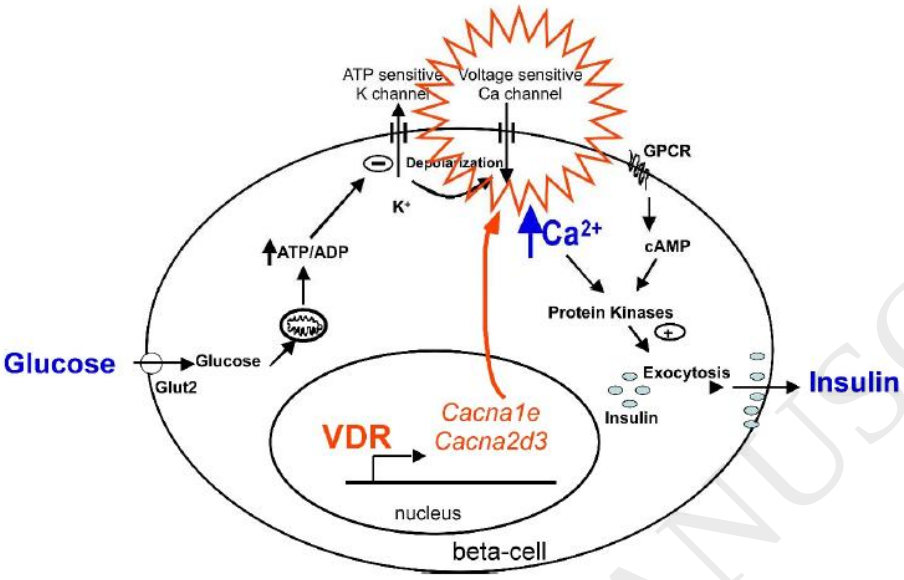

Highlights:

- The vitamin D receptor (VDR, NR1I1) is expressed in pancreatic islets
- 1,25-dihydroxyvitamin-D3 (1,25-D3) enhances GSIS in mouse and human islets
- 1,25- D3 enhances the glucose-stimulated rise in islet cytosolic calcium
- The *cacna1e* gene (encoding the Cav2.3 subunit of the R-type voltage-gated calcium
- channel) is a novel VDR target gene in mouse and human islets

Abstract

Aim: Vitamin D deficiency in rodents negatively affects glucose-stimulated insulin secretion (GSIS) and human epidemiological studies connect poor vitamin D status with type 2 diabetes. Previous studies performed primarily in rat islets have shown that vitamin D can enhance GSIS. However the molecular pathways linking vitamin D and insulin secretion are currently unknown. Therefore, experiments were undertaken to elucidate the transcriptional role(s) of the vitamin D receptor (VDR) in islet function.

Methods: Human and mouse islets were cultured with vehicle or 1,25-dihydroxyvitamin-D_3 ($1,25D_3$) and then subjected to GSIS assays. Insulin expression, insulin content, glucose uptake and glucose-stimulated calcium influx were tested. Microarray analysis was performed. *In silico* analysis was used to identify VDR response elements (VDRE) within target genes and their activity was tested using reporter assays.

Results: *Vdr* mRNA is abundant in islets and *Vdr* expression is glucose-responsive. Preincubation of mouse and human islets with $1,25D_3$ enhances GSIS and increases glucose-stimulated calcium influx. Microarray analysis identified the R-type voltage-gated calcium channel (VGCC) gene, *Cacna1e*, which is highly upregulated by $1,25D_3$ in human and mouse islets and contains a conserved VDRE in intron 7. Results from GSIS assays suggest that $1,25D_3$ might upregulate a variant of R-type VGCC that is resistant to chemical inhibition.

Conclusion: These results suggest that the role of $1,25D_3$ in regulating calcium influx acts through the R-Type VGCC during GSIS, thereby modulating the capacity of beta cells to secrete insulin.

Abbreviations: $1,25D_3$, 1α,25-dihydroxyvitamin D_3; GSIS, glucose-stimulated insulin secretion; RXR, Retinoid X receptor; SAB, secretion assay buffer; VDR. Vitamin D receptor; VDRE, vitamin D response element; VGCC, voltage-gated calcium channel;

Keywords: islet, insulin secretion, vitamin D, calcitriol, voltage-gated calcium channels, transcriptional regulation

1. Introduction

Vitamin D has long been known to be important for proper bone health and regulation of serum calcium and phosphate levels. However, it is becoming more apparent that vitamin D has a much broader role in physiology, affecting immune function, muscle strength, cancer progression, cardiovascular health and diabetes [2, 3]. Publications related to vitamin D and diabetes include epidemiological studies which show an inverse association between vitamin D levels and glucose intolerance [4-7]. Furthermore, several longitudinal observational studies show that vitamin D-deficient subjects have higher risk of developing type 2 diabetes [8-10]. Despite this, outcomes from intervention studies using vitamin D supplementation are less consistent; several clinical studies have reported improved glycemic control following vitamin D supplementation, but others have shown no added beneficial effect on blood glucose levels after vitamin D supplementation ([11], and reviewed in [12-16]). This discrepancy might be partially explained by the genetic variance in the vitamin D receptor (VDR, NR1I1), as improvement in glycemic control after vitamin D supplementation varies depending on VDR genotype [17].

Data from rodent studies support the hypothesis that vitamin D is important for beta-cell health. Vitamin D deficiency has been shown to have unfavorable effects on insulin secretion in rat islets of Langerhans [18, 19]. Studies of insulin secretion using mice lacking VDR have shown conflicting results (reviewed in [20]) as these mice exhibit phenotypes that complicate analysis of islet function and glucose metabolism (alopecia, increased energy expenditure, hypocalcemia and altered levels of hormones such as FGF23, Klotho, and of the renin-angiotensin system). However, in limited studies that have corrected some of these phenotypes by the feeding of rescue diets enriched with calcium, phosphorus, and lactose,

insulin secretion capacity is found to be reduced in *Vdr*-null mice [21] in a manner independent of FGF23 [22] or klotho [23].

To overcome the complications encountered with *in vivo* studies, many experiments have been performed using isolated islets. By this approach, pharmacologic and/or genetic modifications can be limited to the endocrine pancreas, and molecular mechanisms regulating hormone secretion can be directly assessed. However, it must be recognized that isolated islets have some drawbacks, as they lack intact vascularization and innervation. Vitamin D treatment of isolated rat islets has positive effects on glucose-stimulated insulin secretion (GSIS) [24-27], particularly in islets from vitamin D-deficient subjects [18, 24, 28]. In a beautiful report from Billaudel and colleagues it was shown that $1,25D_3$ preincubation of islets from vitamin D-deficient rats resulted in enhanced first- and second-phase insulin secretion upon high-glucose exposure [24]. These changes were coincident to altered calcium flux [24] and dependent on sufficient extracellular calcium [28]. Importantly, these changes in GSIS and calcium handling were evident only after a Vit D preincubation of islets for a minimum of 6h, consistent with a timeframe required for the genomic actions of $1,25D_3$.

The active form of vitamin D_3, 1,25-dihydroxyvitamin D_3 ($1,25D_3$), is a ligand for VDR, a member of the nuclear hormone receptor (NHR) family of transcription factors. VDR acts in conjunction with the obligate heterodimer partner, the retinoid X receptor (RXR) to bind DNA motifs (VDREs) and regulate the expression of vitamin D target genes [29-32]. Based on the results of quantitative RNA analyses, our group has shown VDR to be the fourth most abundant NHR in the mouse pancreatic islet and demonstrated VDR mRNA in human islets [1]. Immunolocalization of VDR protein has confirmed the presence of this NHR in beta-cells of human and rat islets [33, 34]. There is even evidence that the 1alpha-hydroxylase necessary for synthesis of the active vitamin D hormone is present in islet cells of the rat [35] and human [36]. Thereby, $1,25D_3$ can alter beta cell function directly by binding to VDR to affect transcription of genes involved in islet biology. It is recognized that $1,25D_3$ can also elicit rapid, non-genomic effects in a variety of cells (reviewed in [37]), but in this study, we evaluated the genomic effects of $1,25D_3$ on islet function and interrogated the islet transcriptome, after $1,25D_3$ treatment. The aim was to identify gene expression changes that could be correlated with improvement in beta cell function and thereby elucidate a molecular mechanism that links VDR activity to insulin secretion.

2. Materials and methods

2.1. Materials

1,25D_3 (>99.0 % by HPLC) and lithocholic acid (LCA) were purchased from Sigma-Aldrich, and were solubilized in tissue-culture grade DMSO. The fluorescent glucose analog 2-NBDG (2-(*N*-(7-nitrobenz-2-oxa-1,3-diazol-4-yl)amino)-2-deoxyglucose) was obtained from Invitrogen/Molecular Probes. Liberase and Collagenase P, used for islet isolation were obtained from Roche. Collagen I and Poly-L-Lysine were purchased from Becton Dickinson (BD) Bioscience and Sigma-Aldrich, respectively. Oligonucleotides were obtained from Integrated DNA Technologies. Real-time PCR reagents were purchased from Applied Biosystems. Guinea pig anti-insulin polyclonal antibody was purchased from DakoCytomation and anti-guinea pig TRITC secondary antibody from Jackson.

2.2 Animals

All tissues and islets were obtained from 3-5-month-old male mice. The *Vdr*$^{-/-}$ mouse strain [38] was generously provided by Marie DeMay (Harvard Medical School); and had been backcrossed for greater than 10 generations onto an A129/SvEv background. All mice were generated from heterozygote matings, and were genotyped by PCR to identify *Vdr*$^{-/-}$ and *Vdr*$^{+/+}$ (wildtype) littermates for study. Mice were housed in a temperature-controlled room (23 ± 1°C) on a 12-h light (0700 h–1900 h), 12-h dark cycle with *ad libitum* access to water and a standard rodent diet (Harlan Teklad Diet no. 2016, which is supplemented by the manufacturer with 1.5 IU/g Vitamin D_3, resulting in daily consumption of a minimum of 7 IU/day/mouse based on food intake), in cages containing sanitized wood-chip bedding.

A single cohort of 3 month-old *Vdr*$^{+/+}$ male mice (n=3) was anesthetized using mouse cocktail, exsanguinated via the vena cava, and dissected to provide tissues for RNA analyses. Intestinal mucosae were scraped from the proximal third (duodenum), medial third (jejunum) and distal third (ileum) segments of the small bowel for RNA.

All animal work described in this manuscript was approved and conducted under the oversight of the UT Southwestern Institutional Animal Care and Use Committee, which uses the "Guide for the Care and Use of Laboratory Animals" when establishing animal research standards.

2.3 Cell culture

The mouse insulinoma cell line Beta-TC-6 (CRL-11506), the adenoma-derived mouse glucagonoma cell line alpha-TC1-clone 9 (CRL-2350), and human kidney cell line HEK293 (CRL-1573) were obtained from American Type Tissue Culture. The MIN6 mouse insulinoma cell line was kindly

provided by Melanie Cobb (UT Southwestern Medical Center). Cells were maintained in their optimal culture conditions as previously described [1].

MIN6 cells were cultured in complete medium (DMEM, 4mM L-glutamine, 1 mM sodium pyruvate, and 10% heat-inactivated FBS) containing low-glucose (3mM) for 24h, medium was removed and replaced with high-glucose (25 mM) complete medium for various times. Medium was removed, and cells were lysed by addition of RNA-Stat60 for RNA isolation (further described below).

2.4 Mouse Islet isolation

The mouse islet isolation method has been previously described [1]. Briefly, the mouse pancreas was perfused and digested with Liberase RI or Collagenase P enzymes. Islets were then isolated using Ficoll gradient centrifugation and hand-selection under a stereomicroscope for transfer to RPMI 1640 medium (11.1 mM glucose) supplemented with 10% (vol/vol) heat-inactivated fetal bovine serum (FBS), 100 IU/ml penicillin, and 100 μg/ml streptomycin (Invitrogen, Carlsbad, CA). Islets were allowed to recover overnight (37°C, 5% CO_2), with gentle rocking to prevent adherence to culture plates and facilitate subsequent transfer to novel media conditions, as further described in figure legends.

2.5 Mouse islet glucose-stimulated insulin secretion

Islets were pre-incubated in 1,25D_3 (or vehicle, DMSO at 0.1% v/v) for 16 hours in 11 mM glucose medium unless otherwise stated. Islets were then conditioned for 1 hour at 37°C in secretion assay buffer (SAB): pH 7.4, containing 114 mM NaCl, 4.7 mMKCl, 1.2 mM KH_2PO_4, 1.16 mM $MgSO_4$, 2.5 mM $CaCl_2$, 25.5 mM $NaHCO_3$, 20 mM HEPES and 0.2% BSA.. Subsequently, 10 islets per well (4-6 wells per treatment) were incubated for 60 min in SAB containing either low (2.5 or 5 mM) or high (17.5 mM) glucose. The media and islets from this final incubation were collected, and insulin content was measured using a rat sensitive insulin radioimmunoassay (Millipore). Note, 1,25D_3 was not included during the 1h conditioning period nor the 1h insulin secretion collection. Thus our 1,25D_3 treatment strategy (longer preincubation period and absence of ligand during acute (GSIS) phase) was selected to favor identification of genomic effects of vitamin D/VDR.

2.6 Human islet glucose-stimulated insulin secretion

Human islet glucose-stimulated insulin secretion measurement has been described elsewhere [39]. Human islets from three independent donors were maintained at 37°C with 5% CO_2 in media composed

of: RPMI 1640, 10% fetal bovine serum, 100 units/ml penicillin and 100 µg/ml streptomycin. Approximately 50 islets/well were preincubated in 20 nM 1,25D3 or vehicle for 16h, then transferred to Krebs-Ringer buffer, pH 7.4, containing 134 mM NaCl, 4.7 mM KCl, 1.2 mM KH_2PO_4, 1.2 mM $MgSO_4$, 1.0 mM $CaCl_2$, 5 mM $NaHCO_3$, 10 mM HEPES, 0.1% BSA and 2.5 mM (low glucose) or 25 mM (high glucose) for one hour. Culture media were obtained and islets collected for determination of insulin content using an ELISA (Alpco).

2.7 Human islets, microarray analysis

Human pancreatic islets were obtained from a cadaveric donor (49 yo Caucasian male, islet purity at 90%) and immediately placed in RPMI medium containing 11 mM glucose and 10% FBS. Islets (200/well, n=2 per treatment) were then cultured for 16h in the presence of 20 nM $1,25D_3$ or vehicle (DMSO). Total RNA was isolated, and microarray analysis was performed using the Human Affymetrix U133 Plus 2.0 array platform. Comparative gene expression was performed using GeneSifter and Partek software with fold-change cut-off at ≥2 and significant differences set at $p \leq 0.05$. Further interrogation of the microarray data was performed using Ingenuity Pathway Analysis software.

2.8 Total islet insulin

Mouse islets were suspended in 100 µl phosphate-buffered saline (PBS) and sonicated using a Bioruptor XL sonicator (Diagenode). Samples were diluted 1000-fold to assure that insulin levels fell within the linear range of a Rat Sensitive Insulin RIA (Millipore)

2.9 Total pancreatic insulin content in mice receiving vitamin D treatment

Male mice, 3-5 months of age, were assigned to one of the following four treatment groups: wild-type vehicle-injected; wild-type $1,25D_3$-injected; *Vdr*$^{-/-}$ vehicle-injected; and *Vdr*$^{-/-}$ $1,25D_3$-injected (n=7/group). Every other day over a 5-day period, mice received $1,25D_3$ or vehicle (ip injection, $1,25D_3$ at 0.5 ng/g body weight). Twelve hours following the last injection, mice were euthanized, and the pancreas was removed, weighed and placed in acidic ethanol (75% ethanol, 0.2M HCl) on ice. Thereafter, pancreata were homogenized and kept at 4°C overnight. The pancreatic slurry was centrifuged, the supernatant was collected and stored at -20°C, the remaining slurry was homogenized again in a fresh solution of acidic ethanol and kept at 4°C overnight. This process was repeated and all three supernatant extractions for each sample were pooled and diluted 10,000-fold for measuring insulin using a Rat

Sensitive Insulin RIA (Millipore).

2.10 Quantitative real-time PCR (qPCR) measurement of RNA

RNA was isolated from tissue samples, cultured islets or cell lines using RNA STAT-60 (Tel-Test Inc., Friendswood, TX), and reverse-transcribed with random hexamers using SuperScript II (Invitrogen), as previously described in detail [40]. qPCR was performed using an Applied Biosystem Prism 7900HT sequence detection system (Applied Biosystems, Foster City, CA) and SYBR-green chemistry. Gene-specific primers were designed using D-LUX primer design software (www.invitrogen.com) and validated by analysis of template titration and dissociation curves. Primer sequences are provided in the Supplementary Table 1. Multiple housekeeping genes were evaluated in each assay to ensure that these RNA levels were invariant under the experimental conditions of each study. Results of qPCR were evaluated by the comparative Ct method using hypoxanthine-guanine phosphoribosyl transferase (*Hprt*) and cyclophilin as housekeeping control genes.

2.11 Glucose uptake assay

A 96-well plate was prepared by incubating for 1 hour at 37°C with 50 µl/well of a solution containing 10µg/mL Collagen I and 0.1 mg/mL Poly-L-Lysine. Mouse islets were dispersed into single cells by 20 minute incubation in Accutase (Innovative Cell Technologies) at ambient temperature. Dispersed islet cells were washed once with culture media and seeded at 40,000 cells/well. $1,25D_3$ (20 nM) or vehicle (DMSO, 0.1% v/v) was added to wells. 16 hours later, cells were washed with secretion assay buffer (SAB, lacking glucose) and then exposed to the fluorescent glucose analog 2-NBDG (2-deoxy-2-[(7-nitro-2,1,3-benzoxadiazol-4-yl)amino]-D-glucose), 500 µM for 0, 2, 4, 6, or 8 minutes. The plate was rapidly chilled on ice and washed with ice-cold SAB buffer to stop 2-NBDG uptake into cells. Fluorescent imaging was performed with the BD pathway 855 Bioimaging system using a FITC filter, 10x objective and 4x4 montages. After imaging, cells were post-fixed with 4% formaldehyde for 15 minutes, blocked for 1 hour at RT with PBS containing 5% goat serum and 5% donkey serum, and then subjected to immunostaining using a guinea pig anti-Insulin primary antibody (1:300) and anti-guinea pig TRITC secondary antibody (1:300). The plate was returned to the BD pathway 855 Bioimaging system for identification of TRITC-positive beta-cells, and 2-NBDG/FITC data were selected for analysis only from this subset of islet cells. More than 100 cells per group met this criterion for a given experiment, and results were confirmed in two independent experiments.

2.12 Intracellular Calcium measurement

As described above and previously [41], dispersed islet cells were plated on a 96-well plate pre-coated with Collagen I and Poly-L-Lysine. After 16 hour incubation in 20 nM $1,25D_3$ or vehicle, cells were loaded with 5μM Fura-2 AM for 1 hour (37°C and 5% CO2). The cells were then washed with KRH buffer (119 mM NaCl, 4.7 mM KCl, 2.5 mM CaCl, 1.2 mM $MgCl_2$, 1.2 mM KH_2PO_4, 10 mM HEPES, 2.0 mM D-Glucose) and 100μl/well of KRH was added. Intracellular calcium was monitored with the BD pathway 855 Bioimaging system (at 37°C), using a 10x objective and 4x4 montages. Six images were collected at baseline (2 mM glucose) and then 25 μL of 0.092 M glucose in KRH was injected into each well for a final concentration of 20 mM glucose. Images were collected for the following 8 minutes and 25 μl 0.156 M KCl was then injected for a final concentration of 30 mM KCl and images were collected for another 1.5 minutes. After imaging, cells were fixed and stained with insulin as described above. Single cells that stained positive for insulin, had stable baseline and responded to the addition of glucose and KCl were selected for graphing. Over 150 cells/group met these criteria for each experiment, and results were confirmed in three independent experiments.

2.13 Cell reporter assays

Plasmids: The expression plasmids pCMX-mouseVDR and pCMX-mouseRXRα, and the pCMX-β-galactosidase plasmid (used to control for transfection efficiency) were obtained from David Mangelsdorf (UT Southwestern Medical Center). Putative Vitamin D response elements (VDRE) within novel VDR target genes were identified using the algorithm, NHR-scan [42]. Oligonucleotides containing these putative VDRE sites, as well as the positive control VDRE of the mouse *Cyp24a1* promoter, were annealed and subcloned into the HindIII site upstream of the thymidine kinase promoter of the luciferase plasmid, pTK-LUC [43]. Plasmid construction was confirmed by DNA sequencing, and plasmids containing two copies each of the respective VDRE were chosen for use in transfection experiments. Oligonucleotide sequences for VDREs are available in Supplementary Table 2.

Transfections: HEK-293 cells were seeded into a 96-well plate and allowed to reach ~80% confluence. Cells in each well were transfected with 40 ng pCMX-VDR, 20 ng pCMX-RXR, 15 ng pCMX-β-Gal, and 75 ng luciferase reporter plasmid, using Lipofectamine 2000 (Invitrogen). 6 hours later, vehicle (DMSO) or 20 nM $1,25D_3$ was added at a final volume of 0.1%. 24 h after ligand addition, cells were harvested, and analyzed for luciferase (FLUOstar OPTIMA, BMG Labtech) and β-galactosidase

(PowerWave XS, BioTek) activity. Results are expressed as relative luciferase units (RLU), following correction for transfection efficiency using β-gal activity.

2.14 Statistics

All results are expressed as the means ± SEM for each treatment group. Two-tailed Student's *t*-tests were performed to compare differences between two groups. 1-way and 2-way ANOVA, with Bonferroni's multiple comparisons post-test, were used to compare samples in experiments with 3 or more groups. If unequal variance among groups was evident by Bartlett's Test, data were log-transformed before analysis. (In all cases log transformation was sufficient to achieve this goal.) All statistical tests were performed using GraphPad Prism 5 software (GraphPad, San Diego, CA). Significance was established at $P < 0.05$ and is represented with asterisks or symbols for comparison between two groups, or by letter to denote significant differences among multiple groups.

3 **Results**

3.1. VDR is highly expressed in mouse islets and is upregulated by incubation in high glucose.

To determine whether VDR expression in islets is comparable to its expression in traditional vitamin D-responsive tissues such as intestine and kidney, we measured *Vdr* mRNA levels in an array of mouse tissues (Fig. 1A). As expected *Vdr* mRNA levels are most abundant in kidney and small intestine, however, *Vdr* expression is also quite high in islets. All other tissues tested had negligible amounts of *Vdr* mRNA when compared to islets, kidney and small intestine. Next, we examined if islet *Vdr* mRNA levels are sensitive to changes in glucose concentration, as that might suggest that VDR has a role in adaptation of islets to elevated blood glucose levels. We found that *Vdr* expression in isolated mouse islets

increased when glucose levels were elevated in the culture media for 16 hours (Fig. 1B). To confirm and extend these findings, a time-course study was performed using the Min6 insulinoma cell line (Fig. 1C) which showed that *Vdr* mRNA levels are significantly elevated by 3 hours after exposing these cells to high-glucose.

3.2 Vitamin D induces insulin secretion in mouse and human islets.

To evaluate $1,25D_3$ effects on insulin secretion, a GSIS assay was performed on mouse islets pretreated with various doses of $1,25D_3$ (Fig. 2A). $1,25D_3$-pretreated islets show a trend towards increased insulin secretion using a concentration of $1,25D_3$ as low as 0.2 nM, and pretreatment with 2 nM or 20 nM

of $1,25D_3$ results in doubling of insulin secretion. Importantly, no effect of $1,25D_3$ was observed under low-glucose conditions. Furthermore, this $1,25D_3$-enhanced GSIS is entirely dependent on the presence of VDR as the vitamin D hormone fails to enhance GSIS in *Vdr*$^{-/-}$ islets (Fig. 2B). Additionally, pretreatment with the bile acid lithocholic acid (LCA), another physiological ligand for VDR [44], results in elevated GSIS in *wild-type* islets and that induction is blunted in *Vdr*$^{-/-}$ islets (Fig. 2C). The LCA-induced GSIS, not dependent on VDR, is likely due to other bile acid receptors present in islets (Chuang, Kjalarsdottir and Repa, unpublished data). It is noteworthy that *Vdr*$^{-/-}$ islets (Fig 2B and C) exhibit elevated GSIS, which is likely caused by adaptive changes due to lifelong exposure to hypocalcemia in this animal model. The important finding in these studies, however, is that ectopic $1,25D_3$ added in culture fails to enhance GSIS in the absence of VDR. Finally, the design of these studies (using a 16h $1,25D_3$ preincubation followed by 2h of $1,25D_3$-free conditions (during low-glucose SAB incubation, and 1h GSIS)) was optimized to detect only the genomic effects of $1,25D_3$/VDR, without contribution by any acute, non-genomic actions of this hormone.

In order to examine if human islets respond to $1,25D_3$ in a similar fashion as mouse islets, a GSIS assay was performed on human islets obtained from cadaveric donors. Isolated human islets from three different donors were independently pretreated with 20 nM $1,25D_3$ or vehicle for 16 hours and then used for a GSIS assay. All three donor islets showed an improvement in beta cell function after $1,25D_3$ pretreatment. Average response between all three donors shows a 2-fold increase in GSIS when human islets were pretreated with $1,25D_3$ (Fig. 2D).

3.3 $1,25D_3$ pretreatment increases glucose-stimulated calcium uptake.

A candidate approach was taken to identify pathways involved in insulin secretion that might be affected by $1,25D_3$. 16 hour treatment of isolated islets in culture using 20 nM $1,25D_3$ caused no changes in islet insulin mRNA levels (Fig. 3A), and no change in islet total insulin content (Fig. 3B). Total pancreatic insulin content was unchanged in mice receiving $1,25D_3$ by repeated intraperitoneal injection (Fig. 3C). Glucose uptake into primary beta cells was unaffected by $1,25D_3$ treatment (Fig. 3D). However, glucose-stimulated calcium uptake by dispersed primary beta cells was significantly augmented by $1,25D_3$ pretreatment (Fig. 3E). The elevation in cytosolic calcium was not observed when the same experiment was performed in calcium-free media which indicates that the elevation of cytosolic calcium is not solely caused by transport from intracellular calcium stores (data not shown).

3.4 Microarray using human islets identifies CaV2.3 as a VDR-regulated gene

$1,25D_3$ enhances GSIS in both mouse and human islets, which suggests that a conserved molecular pathway between mice and humans may exist. To identify VDR target genes in islets, a microarray analysis was performed using RNA from human islets treated with $1,25D_3$ or vehicle. Downstream analyses revealed 300 genes up-regulated 2-fold or greater with $1,25D_3$ (p-value cut-off was set at ≤ 0.05). Ingenuity Pathway Analysis (IPA) was then performed, which identified calcium signaling/transport to be

the most significantly affected canonical pathway (*p*-value of 0.0016). Figure 4 shows ranking of genes that are transcriptionally elevated with $1,25D_3$ treatment and are classified in the Ingenuity Pathway Analysis software as being involved in calcium signaling and transport. As glucose-enhanced calcium influx is increased in $1,25D_3$-pretreated beta cells, we focused on genes involved in transporting calcium into the cell (*CACNA1E*=CaV2.3, *TRPV6* and *CACNB1*). Of these three genes only *Cacna1e* was also upregulated in mouse islets (data not shown). Using qPCR analysis we observed a 5-fold enhancement of *Cacna1e* mRNA in mouse islets (Fig. 5E) and a 4-fold increase of *CACNA1E* mRNA in human islets after 16 hour treatment using 20 nM $1,25D_3$ (data not shown).

3.5 qPCR analyses for all members of the voltage-gated calcium channel family uncover another $1,25D_3$-upregulated gene in mouse islets.

As two members of the voltage-gated calcium channel (VGCC) family were identified in the human islet microarray (*CACNA1E* and *CACNB1*) and only one of them was confirmed to be potentiated by $1,25D_3$ in mouse islets, we decided to perform a comprehensive analysis of all members of this gene family using mouse islets (Fig. 5A-D). This analysis identified another $1,25D_3$-regulated gene, *Cacna2d3*. *Cacna1e* and *Cacna2d3* were upregulated by $1,25D_3$ (represented by overlaid red boxes in Figure 5); while all other genes showed no significant change with $1,25D_3$ incubation. Importantly, modulation of CaV2.3 and Cacna2d3 by $1,25D_3$ is dependent on the presence of VDR (Fig. 5E).

3.6 Voltage-gated calcium channel genes as target genes of VDR.

Cacna1e was the only gene in the VGCC family shown to be upregulated by $1,25D_3$ in both mouse and human islets. Additionally, this upregulation of *Cacna1e* would be consistent with the observation of increased glucose-stimulated calcium influx. Finally, as this gene has been associated with insulin

secretion and type 2 diabetes [45-47] we considered *Cacna1e* to be a possible candidate gene for the 1,25D_3-enhanced GSIS. Therefore, we scanned the *Cacna1e* locus for VDREs using an *in silico* analysis approach [42]. Four potential VDREs were found in the mouse *Cacna1e* locus and five VDREs in the human *CACNA1E* locus (Fig. 6A). Three of these VDREs are conserved between mouse and human, and

are located in intron 7, exon 13 and exon 18. The additional VDRE in mouse is located in intron 25, while the two VDREs unique to human are located in intron 6 and the 3'UTR. Luciferase reporter assays were used to assess the functionality of the identified VDREs (Fig. 6B). Results show that of the three potential conserved VDREs, only the VDRE in intron 7 is functional. Interestingly, two non-conserved VDREs were also observed to be functional, one in mouse intron 25 and the other in the 3'UTR of the human *CACN1E* gene. Furthermore, since we found that the VGCC delta-subunit gene *Cacna2d3* was highly upregulated by 1,25D_3 in mouse islets we also searched for functional VDREs within the *Cacna2d3* locus. Three functional VDREs were found, two in intron 2 and one in the distal 3'UTR (Supplementary Fig. 1).

3.7 1,25D_3 might up-regulate a variant of CaV2.3 that is resistant to chemical inhibition

There are at least three isoforms of the R-type VGCC channel based on permeation and/or pharmacological properties in mouse (and human), despite all containing the channel subunit CaV2.3 (encoded by *Cacna1e*). Of these three R-type channel subtypes, one is resistant to SNX-482 and the other two are inhibited by SNX-482 with slightly different affinities, IC_{50} of 6 nM or 81 nM [48]. To determine whether 1,25D_3-induced upregulation of the *Cacna1e* gene has functional relevance to GSIS, various doses of SNX-482 were used to limit CaV2.3 action (Fig. 7A, B). 10 nM SNX-482 treatment resulted in a 60% inhibition of GSIS in vehicle-treated islets but failed to inhibit GSIS in 1,25D_3-pretreated islets (Fig. 7A, B). Only at an excessive concentration of SNX-482 (1µM) was GSIS affected in 1,25D_3-pretreated islets, although, at 1 µM, SNX-482 is no longer specific to R-type currents since at this dose L-type and N-type currents are also affected [49, 50]. Furthermore, since the VGCC delta-subunit gene *Cacna2d3* was found to be upregulated in mouse islets by 1,25D_3 and CACNA2D3 has been shown to affect activity of both R-type and L-type VGCC [51], we next tested if L-type VGCC were involved in 1,25D_3-enhanced GSIS. The L-type VGCC inhibitor nifedipine partially blocked GSIS in both vehicle and 1,25D_3-pretreated islets but failed to bring the 1,25D_3-enhanced insulin secretion back to control levels (Fig. 7C, D). Thus, our observations suggest that 1,25D_3 treatment affects the R-type VGCC but not the L-type VGCC.

4. Discussion and conclusions

In this report, we show that pretreating mouse and human islets with the VDR ligand $1,25D_3$ increases glucose-stimulated insulin secretion. This effect is observed at hormone levels that span physiologic (serum concentrations in mice and humans of ~0.2 nM [52, 53]) to pharmacologic (cell-based studies routinely use 10-100 nM to assure VDR saturation [54-56]) concentrations. A second structurally distinct VDR ligand, lithocholic acid, was similarly able to enhance GSIS. We also show that *Vdr* is highly expressed in islets, and that its expression level is glucose-responsive, suggesting an increased reliance on Vitamin D signaling when glucose levels rise. Additionally, we find that glucose-stimulated calcium influx is significantly enhanced in islets pretreated with $1,25D_3$. This supports early research on vitamin D actions in isolated islets since elevated glucose-stimulated calcium flux has been previously identified in vitamin D-treated rat islets [28].

To identify a mechanism to account for increased insulin secretion and calcium influx, we performed a microarray analysis of human islets treated with vehicle or $1,25D_3$. Since the mechanism is likely conserved between species, human microarray results were validated using mouse islets. Thereby, we identified the *Cacna1e* gene encoding for the R-type voltage-gated calcium channel (CaV2.3) to be upregulated by $1,25D_3$ in mouse and human islets. CaV2.3 has previously been suggested to be involved in insulin secretion [46] through study of *Cav2.3*-knockout mouse models. Epidemiologic studies in Pima Indians suggest that genetic variants of *CaV2.3* might increase risk of developing type 2 diabetes [47], and it's tempting to speculate that perhaps these could result in calcitriol resistance. Finally, the *CACNA1E* gene is associated with a potent islet enhancer cluster to suggest a role in islet cell identity ane/or function [57].

This prompted us to look at the role of CaV2.3 in $1,25D_3$-enhanced GSIS further. Using an *in silico* approach and cell-reporter assays, we identified a conserved VDRE in intron 7 of the mouse *Cacna1e* and the human *CACNA1E* genes. Finally, GSIS results using the CaV2.3 inhibitor SNX-482 suggest that $1,25D_3$ treatment might cause a shift in CaV2.3 isoforms. There are at least three CaV2.3 isoforms, one that is resistant to SNX-482 inhibition, a second that is inhibited by SNX-482 with an IC_{50} of 6 nM, and a third isoform with an IC_{50} of 81 nM [48]. Our results suggest that the CaV2.3 isoform present in vehicle-treated islets is the IC_{50}=6nM isoform, but treatment with $1,25D_3$ modifies gene expression to alter the complement of isoforms for CaV2.3 to enhance the subtype that is resistant to SNX-482. Another subunit, *Cacna2d3*, was highly $1,25D_3$-responsive in mouse islets. Upregulation of *Cacna2d3* adds further complexity to $1,25D_3$-enhanced GSIS, as CACNA2D3 has been shown to increase current density of both

CaV1.2 and CaV2.3 channels [51]. We addressed this by using the L-type VGCC inhibitor nifedipine and found that L-type VGCC were unaffected by $1,25D_3$ treatment. Further investigations are warranted to examine how $1,25D_3$ affects electrophysiological properties of mouse and human beta cells. Since it is unlikely that *Cacna1e* is the only gene induced by $1,25D_3$ in mouse and human islets, future experiments are underway where we will compare microarrays from $1,25D_3$-treated human and mouse islets. These studies could provide us with a number of other genes that might further increase our understanding of the actions of VDR in islet biology.

Overall, this work extends previous findings using rat islets, to demonstrate that mouse and human islets also respond to the hormone, $1,25D_3$, to enhance glucose-stimulated insulin secretion from the endocrine pancreas. The study designs we employed suggest that transcriptional regulation by VDR increases expression of voltage-gated calcium channels to promote insulin exocytosis from the beta-cell under high-glucose conditions. These findings suggest that optimal vitamin D levels and/or vitamin D supplementation may provide an important adjuvant therapy for diabetes.

Competing interest statement

The authors declare that they have no conflicts of interest

Acknowledgements

The authors wish to thank, from UT Southwestern Medical Center: Yingfeng Deng and Philipp Scherer for assistance with microarray analysis; and Brock McNeal and Ernest Tong for technical assistance. Finally we would like to thank Hans Hohmeier and Mette Jensen (Duke University) and Finnbogi Thormodsson (ValaMed, Reykjavik, Iceland) for their comments and suggestions. This work was supported by grants from the American Diabetes Association (7-04-RA-94 and 7-13-BS-143 to JJR).

References

[1] Chuang J-C, Cha J-Y, Garmey JC, Mirmira RG, and Repa JJ, Nuclear hormone receptor expression in the endocrine pancreas., Mol. Endocrinol. 22 (2008) 2353-2363. doi: 10.1210/me.2007-0568

[2] Wang S, Epidemiology of vitamin D in health and disease., Nutr. Res. Rev. 22 (2009) 188-203. doi: 10.1017/S0954422409990151

[3] Zittermann A, and Gummert JF, Nonclassical vitamin D actions., Nutrients 2 (2010) 408-425. doi: 10.3390/nu2040408

[4] Ford ES, Zhao G, Li C, and Pearson WS, Serum concentrations of vitamin D and parathyroid hormone and prevalent metabolic syndrome among adults in the United States., J. Diabetes 1 (2009) 296-303. doi: 10.1111/j.1753-0407.2009.00046.x

[5] Kositsawat J, Freeman VL, Gerber BS, and Geraci S, Association of A1C levels with vitamin D status in U.S. adults., Diabetes Care 33 (2010) 1236-1238. doi: 10.2337/dc09-2150

[6] Mitri J, Nelson J, Ruthazer R, Garganta C, Nathan DM, Hu FB, Dawson-Hughes B, Pittas AG, and Group DPPR, Plasma 25-hydroxyvitamin D and risk of metabolic syndrome: an ancillary analysis in the Diabetes Prevention Program., Eur. J. Clin. Nutr. 68 (2014) 376-383. doi: 10.1038/ejcn.2013.293

[7] Zhao G, Ford ES, and Li C, Associations of serum concentrations of 25-hydroxyvitamin D and parathyroid hormone with surrogate markers of insulin resistance among U.S. adults without physician-diagnosed diabetes: NHANES, 2003-2006., Diabetes Care 33 (2010) 344-347. doi: 10.2337/dc09-0924

[8] Anderson JL, May HT, Horne BD, Bair TL, Hall NL, Carlquist JF, Lappe DL, and Muhlestein JB, Relation of vitamin D deficiency to cardiovascular risk factors, disease status, and incident events in a general healthcare population., Am. J. Cardiol. 106 (2010) 963-968. doi: 10.1016/j.amjcard.2010.05.027

[9] Knekt P, Laaksonen M, Mattila C, Harkanen T, Marniemi J, Heliovaara M, Rissanen H, Montonen J, and Reunanen A, Serum vitamin D and subsequent occurence of type 2 diabetes., Epidemiology 19 (2008) 666-671. doi: 10.1097/EDE.0b013e318176b8ad

[10] Pittas AG, Sun Q, Manson JE, Dawson-Hughes B, and Hu FB, Plasma 25-hydroxyvitamin D concentration and risk of incident type 2 diabetes in women., Diabetes Care 33 (2010) 2021-2023.doi: 10.2337/dc10-0790

[11] Park SK, Garland CF, Gorham ED, BuDoff L, and Barrett-Connor E, Plasma 25-hydroxyvitamin D concentration and risk of type 2 diabetes and pre-diabetes: 12-year cohort study., PLoS One 13 (2018) e0193070. doi: 10.1371/journal.pone.0193070

[12] Lucato P, Solmi M, Maggi S, Bertocco A, Bano G, Trevisan C, Manzato E, Sergi G, Schofield P,

Kouidrat Y, Veronese N, and Stubbs B, Low vitamin D levels increase the risk of type 2 diabetes in older adults: A systematic review and metab-analysis., Maturitas 100 (2017) 8-15. doi: 10.1016/j.maturitas.2017.02.016

[13] Lips P, Eekhoff M, van Schoor N, Oosterwerff M, de Jongh R, Krul-Poel Y, and Simsek S, Vitamin D and type 2 diabetes., J. Steroid Biochem. Mol. Biol. 173 (2017) 280-285. doi: 10.1016/j.jsbmb.2016.11.021

[14] Mitri J, and Pittas AG, Vitamin D and diabetes., Endocrinol. Metab. Clin. N. Am. 43 (2014) 205-232. doi: 10.1016/j.ecl.2013.09.010

[15] Takiishi T, Gysemans C, Bouillon R, and Mathieu C, Vitamin D and diabetes., Rheum. Dis. Clin. N. Am. 38 (2012) 179-202. doi: 10.1016/j.rdc.2012.03.015

[16] Seida JC, Mitri J, Colmers IN, Majumdar SR, Davidson MB, Edwards AL, Hanley DA, Pittas AG, Tjosvold L, and Johnson JA, Effect of vitamin D_3 supplementation on improving glucose homeostasis and preventing diabetes: a systematic review and meta-analysis., J. Clin. Endocrinol. Metab. 99 (2014) 3551-3560. doi: 10.1210/jc.2014-2136

[17] Al-Daghri NM, Mohamme AK, Al-Attas OS, Ansari MGA, Wani K, Hussain SD, Sabico S, Tripathi G, and Alokail MS, Vitamin D receptor gene polymorphisms modify cardiometabolic response to vitamin D supplementation in T2DM patients., Sci. Rep. 7 (2017) 8280. doi: 10.1038/s41598-017-08621-7

[18] Cheng Q, Boucher BJ, and Leung PS, Modulation of hypovitaminosis D-induced islet dysfunction and insulin resistance through direct suppression of the pancreatic islet renin-angiotensin system in mice., Diabetologia 56 (2013) 553-562. doi: 10.1007/s00125-012-2801-0

[19] Norman AW, Frankel JB, Heldt AM, and Grodsky GM, Vitamin D deficiency inhibits pancreatic secretion of insulin., Science 209 (1980) 823-825. doi: 10.1126/science.6250216

[20] Bouillon R, Carmeliet G, Verlinden L, van Etten E, Verstuyf A, Luderer HF, Lieben L, Mathieu C, and Demay M, Vitamin D and human health: lessons from vitamin D receptor null mice., Endocrine J. 29 (2008) 726-776. doi: 10.1210/er.2008-0004

[21] Zeitz U, Weber K, Soegiarto DW, Wolf E, Balling R, and Erben RG, Impaired insulin secretory capacity in mice lacking a functional vitamin D receptor., FASEB J. 17 (2003) 509-511. doi: 10.1096/fj.02-0424fje

[22] Streicher C, Zeitz U, Andrukhova O, Rupprecht A, Pohl EE, Larsson TE, Windisch W, Lanske B, and Erben RG, Long-term *Fgf23* deficiency does not influence aging, glucose homeostasis, or fat metabolism in mice with a nonfunctionaing vitamin D receptor., Endocrinology 153 (2012) 1795-1805. doi: 10.1210/en.2011-1878

[23] Anour R, Andrukhova O, Ritter E, Zeitz U, and Erben RG, Klotho lacks a vitamin D independent physiological role in glucose homeostasis, bone turnover, and steady-state PTH secretion *in vivo*.,

PLoS One 7 (2012) e31376. doi: 10.1371/journal.pone.0031376

[24] Billaudel BJL, Faure AG, and Sutter BCJ, Effect of 1,25 dihydroxyvitamin D_3 on isolated islets from vitamin D_3-deprived rats., Am. J. Physiol. 258 (1990) E643-E648. doi: 10.1152/ajpendo.1990.258.4.E643

[25] Bourlon P-M, Billaudel B, and Faure-Dussert A, Influence of vitamin D_3 deficiency and 1,25 dihydroxyvitamin D_3 on *de novo* insulin biosynthesis in the islets of the rat endocrine pancreas., J. Endocrinol. 160 (1999) 87-95. doi: doi: 10.1677/joe.0.1600087

[26] Cade C, and Norman AW, Rapid normalization/stimulation by 1,25-dihydroxyvitamin D_3 of insulin secretion and glucose tolerance in the vitamin D-deficient rat., Endocrinology 120 (1987) 1490-1497. doi: 10.1210/endo-120-4-1490

[27] Jeddi S, Syedmoradi L, Bagheripour F, and Ghasemi A, The effects of vitamin D on insulin release from isolated islets of rats., Int. J. Endocrinol. Metab. 13 (2015) e20620. doi: 10.5812/ijem.20620

[28] Billaudel BJL, Delbancut APA, Sutter BCJ, and Faure AG, Stimulatory effect of 1,25-dihydroxyvitamin D_3 on calcium handling and insulin secretion by islets from vitamin D_3-deficient rats., Steroids 58 (1993) 335-341. doi: https://doi.org/10.1016/0039-128X(93)90094-4

[29] Kim S, Yamazaki M, Zella LA, Meyer MB, Fretz JA, Shevde NK, and Pike JW, Multiple enhancer regions located at significant distances upstream of the transcripitonal start site mediate RANKL gene expression in response to 1,25-dihydroxyvitamin D_3., J. Steroid Biochem. Mol. Biol. 103 (2007) 430-434. doi: 10.1016/j.jsbmb.2006.12.020

[30] Meyer MB, Goetsch PD, and Pike JW, A downstream intergenic cluster of regulatory enhancers contributes to the induction of *CYP24A1* expression by 1α,25-dihydroxyvitamin D_3., J. Biol. Chem. 285 (2010) 15599-15610. doi: 10.1074/jbc.M110.119958

[31] Meyer MB, Goetsch PD, and Pike JW, Genome-wide analysis of the VDR/RXR cistrome in osteoblast cells provides new mechanistic insight into the actions of the vitamin D hormone., J. Steroid Biochem. Mol. Biol. 121 (2010) 136-141. doi: 10.1016/j.jsbmb.2010.02.011

[32] Stoffers KL, Sorg BL, Seuter S, Rau O, Radmark O, and Steinhilber D, Calcitriol upregulates open chromatin and elongation markers at functional vitamin D response elements in the distal part of the 5-lipoxygenase gene., J. Mol. Biol. 395 (2010) 884-896. doi: 10.1016/j.jmb.2009.10.022

[33] Johnson JA, Grande JP, Roche PC, and Kumar R, Immunohistochemical localization of the 1,25$(OH)_2D_3$ receptor and calbinding D_{28k} in human and rat pancreas., Am. J. Physiol. 267 (1994) E356-E360. doi: 10.1152/ajpendo.1994.267.3.E356

[34] Hummel D, Aggarwal A, Borka K, Bajna E, Kallay E, and Horvath HC, The vitamin D system is deregulated in pancreatic diseases., J. Steroid Biochem. Mol. Biol. 144 (2014) 402-409. doi: 10.1016/j.jsbmb.2014.07.011

[35] Bland R, Markovic D, Hills CE, Hughes SV, Chan SLF, Squires PE, and Hewison M, Expression of 25-hydroxyvitamin D_3-1α-hydroxylase in pancreatic islets., J. Steroid Biochem. Mol. Biol. 89-90 (2004) 121-125. doi: 10.1016/j.jsbmb.2004.03.115

[36] Zehnder D, Bland R, Williams MC, McNinch RW, Howie AJ, Stewart PM, and Hewison M, Extrarenal expression of 25-hydroxyvitamin D_3-1α-hydroxylase., J. Clin. Endocrinol. Met. 86 (2001) 888-894. doi: 10.1210/jcem.86.2.7220

[37] Revelli A, Massobrio M, and Tesarik J, Nongenomic effects of 1α,25-dihydroxyvitamin D_3., Trends Endocrinol. Metab. 9 (1998) 419-427. doi: https://doi.org/10.1016/S1043-2760(98)00100-3

[38] Li YC, Pirro AE, Amling M, Delling G, Baron R, Bronson R, and Demay MB, Targeted ablation of the vitamin D receptor: an animal model of vitamin D-dependent rickets type II with alopecia., Proc. Natl. Acad. Sci. USA 94 (1997) 9831-9835. doi: https://doi.org/10.1073/pnas.94.18.9831

[39] Ogihara T, Chuang J-C, Vestermark GL, Garmey JC, Ketchum RJ, Huang X, Brayman KL, Thorner MO, Repa JJ, Mirmira RG, and Evans-Molina C, Liver X receptor agonists augment human islet function through activation of anaplerotic pathways and glycerolipid/free fatty acid cycling., J. Biol. Chem. 285 (2010) 5392-5404. doi: 10.1074/jbc.M109.064659

[40] Kurrasch DM, Huang J, Wilkie TM, and Repa JJ, Quantitative real-time polymerase chain reaction measurement of regulators of G-protein signaling mRNA levels in mouse tissues., Meth. Enzymol. 389 (2004) 3-15. doi: 10.1016/S0076-6879(04)89001-3

[41] Mani BK, Chuang J-C, Kjalarsdottir L, Sakata I, Walker AK, Kuperman A, Osborne-Lawrence S, Repa JJ, and Zigman JM, Role of calcium and EPAC in norepinephrine-induced ghrelin secretion., Endocrinology 155 (2014) 98-107. doi: 10.1210/en.2013-1691

[42] Sandelin A, and Wasserman WW, Prediction of nuclear hormone receptor response elements., Mol. Endocrinol. 19 (2005) 595-606. doi: 10.1210/me.2004-0101

[43] Willy PJ, and Mangelsdorf DJ, Unique requirements for retinoid-dependent transcriptional activation by the orphan receptor LXR., Genes & Dev. 11 (1997) 289-298. doi: 10.1101/gad.11.3.289

[44] Nehring JA, Zierold C, and DeLuca HF, Lithocholic acid can carry out *in vivo* functions of vitamin D., Proc. Natl. Acad. Sci. USA 104 (2007) 10006-10009. doi: 10.1073/pnas.0703512104

[45] Holmkvist J, Tojjar D, Almgren P, Lyssenko V, Lindgren CM, Isomaa B, Tuomi T, Berglund G, Renstrom E, and Groop L, Polymorphisms in the gene encoding the voltage-dependent Ca^{2+} channel $Ca_v2.3$ (*CACNA1E*) are associated with type 2 diabetes and impaired insulin secretion., Diabetologia 50 (2007) 2467-2475. doi: 10.1007/s00125-007-0846-2

[46] Jing X, Li D-Q, Olofsson CS, Salehi A, Surve VV, Caballero J, Ivarsson R, Lundquist I, Pereverzev A, Schneider T, Rorsman P, and Renstrom E, $Ca_v2.3$ calcium channels control second-

phase insulin release., J. Clin. Invest. 115 (2005) 146-154. doi: 10.1172/JCI22518

[47] Muller YL, Hanson RL, Zimmerman C, Harper I, Sutherland J, Kobes S, Knowler WC, Bogardus C, and Baier LJ, Variants in the $Ca_V2.3$ (α1E) subunit of voltage-activated Ca^{2+} channels are associated with insulin resistance and type 2 diabetes in Pima Indians., Diabetes 56 (2007) 3089-3094. doi: 10.2337/db07-0587

[48] Tottene A, Volsen S, and Pietrobon D, α_{1E} Subunits form the pore of three cerebellar R-type calcium channels with different pharmacological and permeation properties., J. Neurosci. 20 (2000) 171-178. doi: https://doi.org/10.1523/JNEUROSCI.20-01-00171.2000

[49] Bourinet E, Stotz SC, Spaetgens RL, Dayanithi G, Lemos J, Nargeot J, and Zamponi GW, Interaction of SNX482 with domains III and IV inhibits activation gating of α_{1E} ($Ca_v2.3$) calcium channels., Biophys. J. 81 (2001) 79-88. doi: 10.1016/S0006-3495(01)75681-0

[50] Newcomb R, Szoke B, Palma A, Wang G, Chen X, Hopkins W, Cong R, Miller J, Urge L, Tarczy-Hornoch K, Loo JA, Dooley DJ, Nadasdi L, Tsien RW, Lemos J, and Miljanich G, Selective peptide antagonist of the class E calcium channel from the venom of the tarantula *Hysterocrates gigas*., Biochemistry 37 (1998) 15353-15362. doi: 10.1021/bi981255g

[51] Klugbauer N, Lacinova L, Marais E, Hobom M, and Hofmann F, Molecular diversity of the calcium channel $\alpha_2\delta$ subunit., J. Neurosci. 19 (1999) 684-691. doi: https://doi.org/10.1523/JNEUROSCI.19-02-00684.1999

[52] Dardenne O, Prud'homme J, Arabian A, Glorieux FH, and St. Arnaud R, Targeted inactivation of the 25-hydroxyvitamin D_3-1α-hydroxylase gene (CYP27B1) creates an animal model of pseudovitamin D-deficiency rickets., Endocrinology 142 (2001) 3135-3141. doi: 10.1210/endo.142.7.8281

[53] Christensen SE, Nissen PH, Vestergaard P, Heickendorff L, Rejnmark L, Brixen K, and Mosekilde L, Plasma 25-hydroxyvitamin D, 1,25-dihydroxyvitamin D, and parathyroid hormone in familial hypocalciuric hypercalcemia and primary hyperparathyroidism., Eur. J. Endocrinol. 159 (2008) 719-727. doi: 10.1530/EJE-08-0440

[54] Kim S, Yamazaki M, Zella LA, Shevde NK, and Pike JW, Activation of receptor activator of NF-κB ligand gene expression by 1,25-dihydroxyvitamin D_3 is mediated through multiple long-range enhancers., Mol. Cell. Biol. 26 (2006) 6469-6486. doi: 10.1128/MCB.00353-06

[55] Jurutka PW, Thompson PD, Whitfield GK, Eichhorst KR, Hall N, Dominguez CE, Hsieh J-C, Haussler CA, and Haussler MR, Molecular and functional comparison of 1,25-dihydroxyvitamin D_3 and the novel vitamin D receptor ligand, lithocholic acid, in activating transcription of cytochrome P450 3A4., J. Cell. Biochem. 94 (2005) 917-943. doi: 10.1002/jcb.20359

[56] Tarroni P, Villa I, Mrak E, Zolezzi F, Mattioli M, Gattuso C, and Rubinacci A, Microarray analysis of $1,25(OH)_2D_3$ regulated gene expression in human primary osteoblasts., J. Cell. Biochem. 113 (2011) 640-649. doi: 10.1002/jcb.23392

[57] Pasquali L, Gaulton KJ, Rodriguez-Segui SA, Mularoni L, Miguel-Escalada I, Akerman I, Tena JJ, Moran I, Gomez-Marin C, van De Bunt M, Ponsa-Cobas J, Castrol N, Nammo T, Cebola I, Garcia-Hurtado J, Maestro MA, Pattou F, Piemonti L, Berney T, Gloyn AL, Ravassard P, Gomez-Skarmeta JL, Muller F, McCarthy MI, and Ferrer J, Pancreatic islet enhancer clusters enriched in type 2 diabetes risk-associated variants., Nature Genet. 46 (2014) 136-143. doi: 10.1038/ng.2870

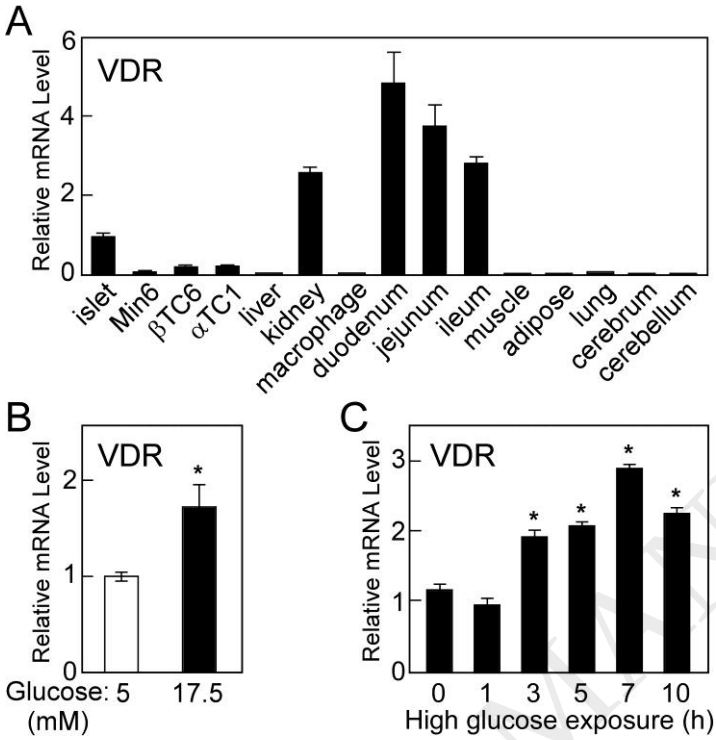

Fig. 1. VDR is expressed in pancreatic islets and is upregulated by high glucose. **A**. Expression levels of VDR mRNA in male A129/Sv mice tissues and mouse cell lines (Min6, βTC6 and αTC1). **B**. Glucose regulation of VDR mRNA levels in mouse islets, cultured in 3 mM glucose for 8 hours, then transferred to media containing low (5 mM) or high (17.5 mM) glucose for 16 hours. **C**. Time course of glucose regulation of VDR mRNA levels in Min6 cells, incubated in 3 mM glucose for 24 hours, then transferred to media containing 25 mM glucose for indicated times prior to RNA isolation and measurement by qPCR. All values depict the mean ± SEM of 3-4 individual samples or cultures. *p<0.05 compared to low-glucose control by Student's t-test (B) or ANOVA (C).

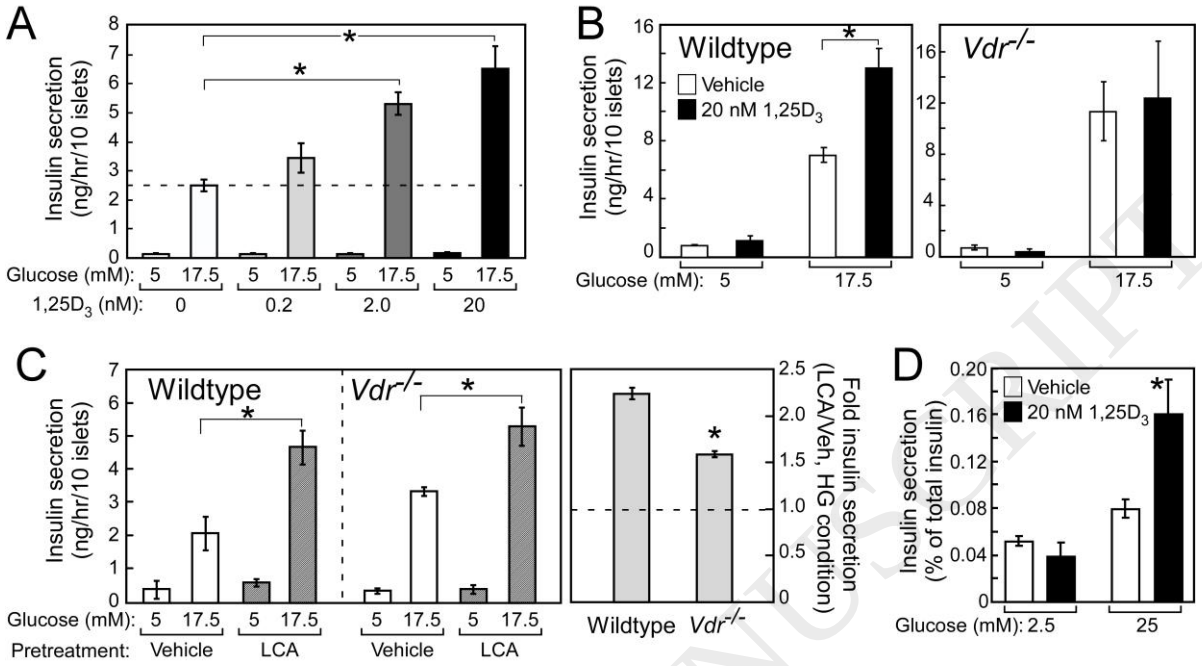

Fig. 2. 1,25D$_3$ enhances GSIS in mouse islets. **A**. Dose-response. Islets isolated from A129/Sv mice were incubated in vehicle (DMSO), 0.2 nM, 2 nM or 20 nM 1,25D$_3$ for 16 hours, then transferred to buffer supplemented with low glucose (5 mM) or high-glucose (17.5 mM) for insulin collection over 1h. **B**. VDR-dependence. Islets isolated from wildtype and *Vdr*$^{-/-}$ mice were incubated in vehicle or 20 nM 1,25D$_3$ for 16 hours and assessed as in (A). **C**. Alternative VDR ligand. Islets from wildtype or *Vdr*$^{-/-}$ mice were pretreated for 16 hours in 10 mM LCA or vehicle prior to GSIS assay as described in (A). **D**. Human islets were exposed to 2.5 or 25 mM glucose for 1 h following a 16 h-preincubation with 1,25D$_3$ (20 nM) or vehicle (DMSO 0.1% v/v), and secreted insulin was measured. Values reflect average of 3 independent experiments using islets from 3 different donors. For **A-D**, all data are shown as the mean ± S.E.M. For simplicity, only significant differences due to VDR ligand pretreatment between high-glucose and vehicle-treated islets is denoted (*, p<0.05).

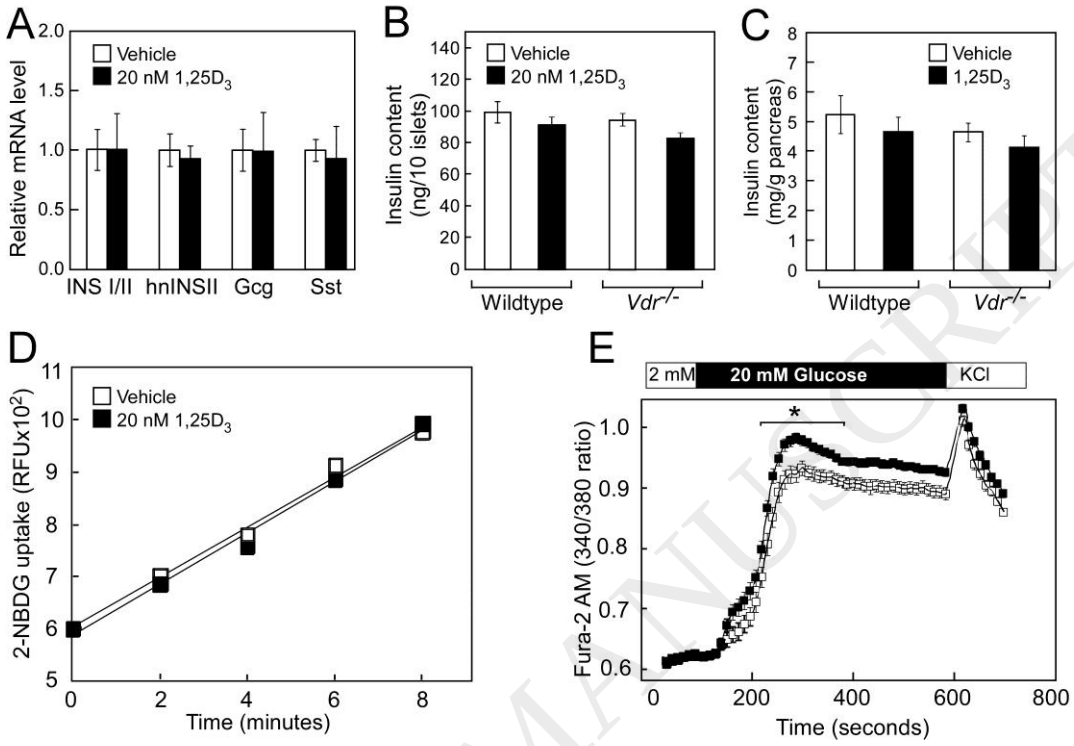

Fig. 3. $1,25D_3$ pretreatment has no effect on hormone expression/content or glucose uptake capacity of islets, but increases glucose-stimulated calcium influx. **A**: mRNA levels of insulin (I&II), insulin II (heterogenous INSII [1]), glucagon (Gcg) and somatostatin (Sst) were measured by qPCR for A129/Sv islets treated for 16h with vehicle (DMSO, 0.1% v/v) or $1,25D_3$ (20 nM). **B**: Insulin content of A129/Sv islets treated for 16h with vehicle or $1,25D_3$ was measured for wildtype and *Vdr*$^{-/-}$ islets. **C**: Wildtype and *Vdr*$^{-/-}$ mice were injected with $1,25D_3$ (0.5ng/g bodyweight, ip) every other day for 5 days and then pancreatic insulin was measured. **D**: Dispersed cells from primary mouse islets were cultured for 16 h in the presence of vehicle or 20 nM $1,25D_3$. Cells were then incubated in 500µM 2-NBDG for 0, 2, 4, 6, or 8 minutes (n=500 cells) and glucose uptake by beta-cells was determined by fluorescence imaging. **E**: Dispersed cells, as in (D) were loaded with FURA-2 AM, glucose was applied to a final concentration of 20 mM, then cells were depolarized using 30 mM KCl. For results of (D) and (E), fluorescent imaging was performed using a BD Pathway 855 Bioimaging system, and analyses were limited to beta-cells identified by post-imaging insulin immunostaining. All data are shown as the mean ± S.E.M. Asterisk denotes a significant difference ($p < 0.05$) between vehicle and $1,25D_3$ treatment calculated using 2-way ANOVA with Bonferroni's multiple comparisons post-test.

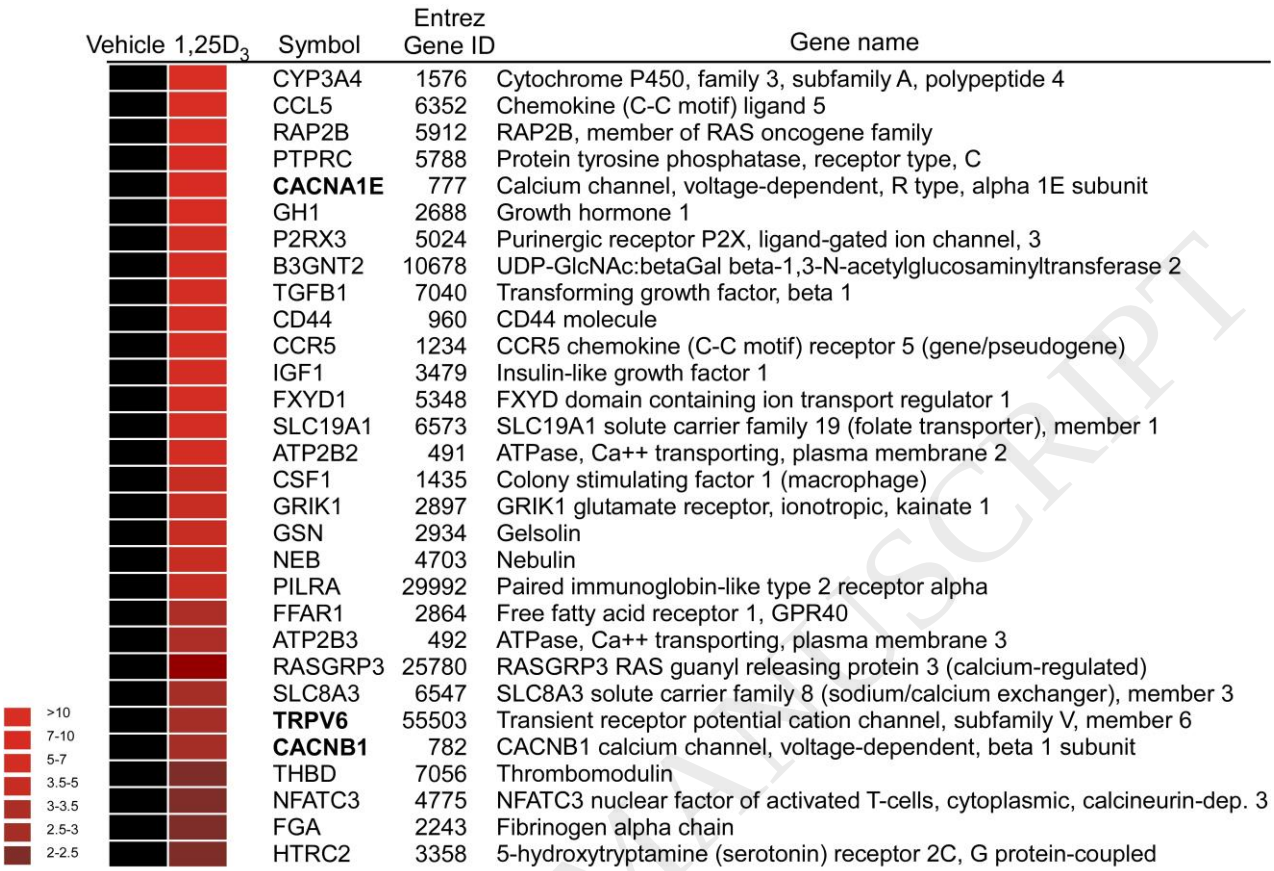

Symbol	Entrez Gene ID	Gene name
CYP3A4	1576	Cytochrome P450, family 3, subfamily A, polypeptide 4
CCL5	6352	Chemokine (C-C motif) ligand 5
RAP2B	5912	RAP2B, member of RAS oncogene family
PTPRC	5788	Protein tyrosine phosphatase, receptor type, C
CACNA1E	777	Calcium channel, voltage-dependent, R type, alpha 1E subunit
GH1	2688	Growth hormone 1
P2RX3	5024	Purinergic receptor P2X, ligand-gated ion channel, 3
B3GNT2	10678	UDP-GlcNAc:betaGal beta-1,3-N-acetylglucosaminyltransferase 2
TGFB1	7040	Transforming growth factor, beta 1
CD44	960	CD44 molecule
CCR5	1234	CCR5 chemokine (C-C motif) receptor 5 (gene/pseudogene)
IGF1	3479	Insulin-like growth factor 1
FXYD1	5348	FXYD domain containing ion transport regulator 1
SLC19A1	6573	SLC19A1 solute carrier family 19 (folate transporter), member 1
ATP2B2	491	ATPase, Ca++ transporting, plasma membrane 2
CSF1	1435	Colony stimulating factor 1 (macrophage)
GRIK1	2897	GRIK1 glutamate receptor, ionotropic, kainate 1
GSN	2934	Gelsolin
NEB	4703	Nebulin
PILRA	29992	Paired immunoglobin-like type 2 receptor alpha
FFAR1	2864	Free fatty acid receptor 1, GPR40
ATP2B3	492	ATPase, Ca++ transporting, plasma membrane 3
RASGRP3	25780	RASGRP3 RAS guanyl releasing protein 3 (calcium-regulated)
SLC8A3	6547	SLC8A3 solute carrier family 8 (sodium/calcium exchanger), member 3
TRPV6	55503	Transient receptor potential cation channel, subfamily V, member 6
CACNB1	782	CACNB1 calcium channel, voltage-dependent, beta 1 subunit
THBD	7056	Thrombomodulin
NFATC3	4775	NFATC3 nuclear factor of activated T-cells, cytoplasmic, calcineurin-dep. 3
FGA	2243	Fibrinogen alpha chain
HTRC2	3358	5-hydroxytryptamine (serotonin) receptor 2C, G protein-coupled

Fig. 4. Microarray analysis identifies numerous genes associated with cellular calcium handling, as potential targets of VDR action in human islets. Human islets were treated with vehicle (DMSO) or 20 nM $1,25D_3$ for 16 hours prior to RNA isolation (n=2 samples per condition). Over 300 genes were found to have RNA levels increased by $\geq$2 fold (p-value cut-off was set at $\leq$ 0.05). The Ingenuity Pathway Analysis software identified calcium signaling to be the most significant canonical pathway and this heat map depicts the 30 most-upregulated genes of this category. The key for fold-change in mRNA levels is provided at the lower left, and the black bars of the vehicle-group represent the basal state (a unit of 1). Of note, all these genes were deemed "present" in both treatment groups.

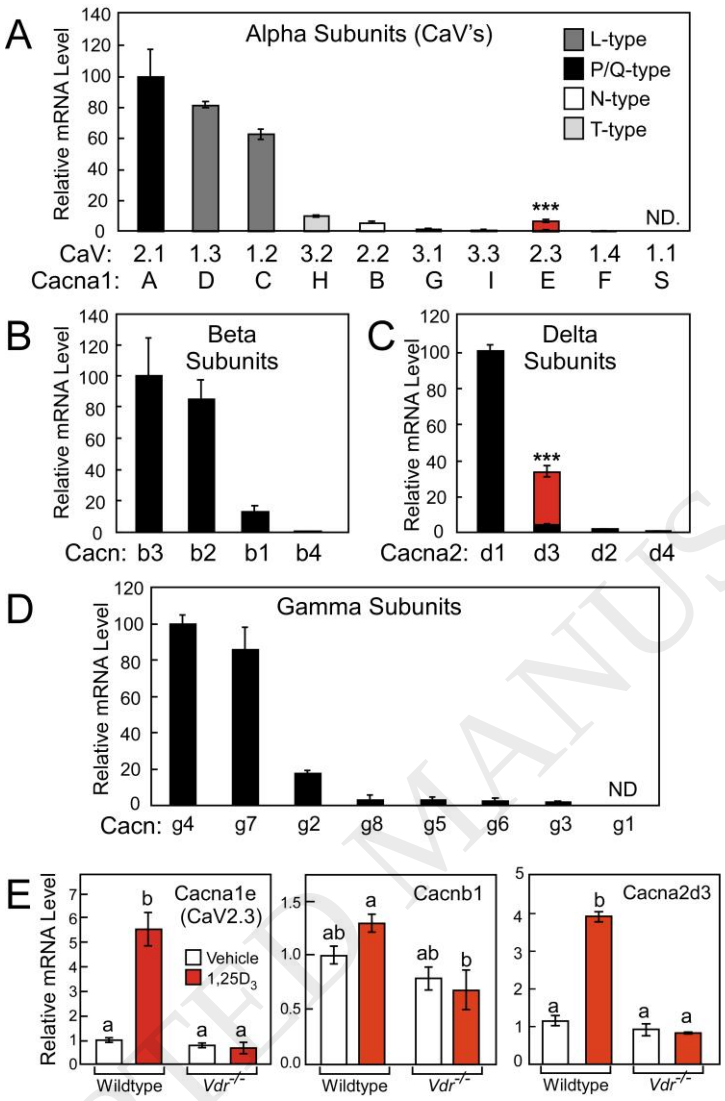

Fig. 5. Gene expression survey for all subunits of the voltage-gated calcium channel family demonstrates that *Cacna1e* (CaV2.3) and *Cacna2d3* are upregulated by $1,25D_3$ in mouse islets. Primary mouse islets were incubated in 20 nM $1,25D_3$ or vehicle (DMSO) for 16 hours before RNA isolation. **A**: Rank order of mRNA levels [gene names on x-axis] for the alpha subunits (transmembrane channels) of voltage-gated calcium channels. These are gray-scaled to denote their classification by pharmacologic inhibitors (L-, P/Q-, N-, T- and R-types). **B**: Rank order of mRNA levels for the beta regulatory subunits. Rank order of mRNA levels of the alpha-2-delta regulatory subunits (**C**) and gamma regulatory subunits **(D**). Overlaid red boxes on CaV2.3 (*Cacna1e*, in panel A) and *Cacna2d3* (in panel C) illustrate up-regulation by $1,25D_3$ in wildtype A129/Sv islets from three independent experiments. E. VDR-dependence in the regulation of CaV2.3 (*Cacna1e*) and *Cacna2d3* expression is revealed by increased mRNA levels observed only in wildtype, not $Vdr^{-/-}$, mouse islets. All data are shown as the mean ± S.E.M. (n = 4). ***p<0.005 (panels A and C) as determined by Student's t-test. Data of panel **E** were analyzed by ANOVA and bars identified by unique letters are significantly different (p<0.05).

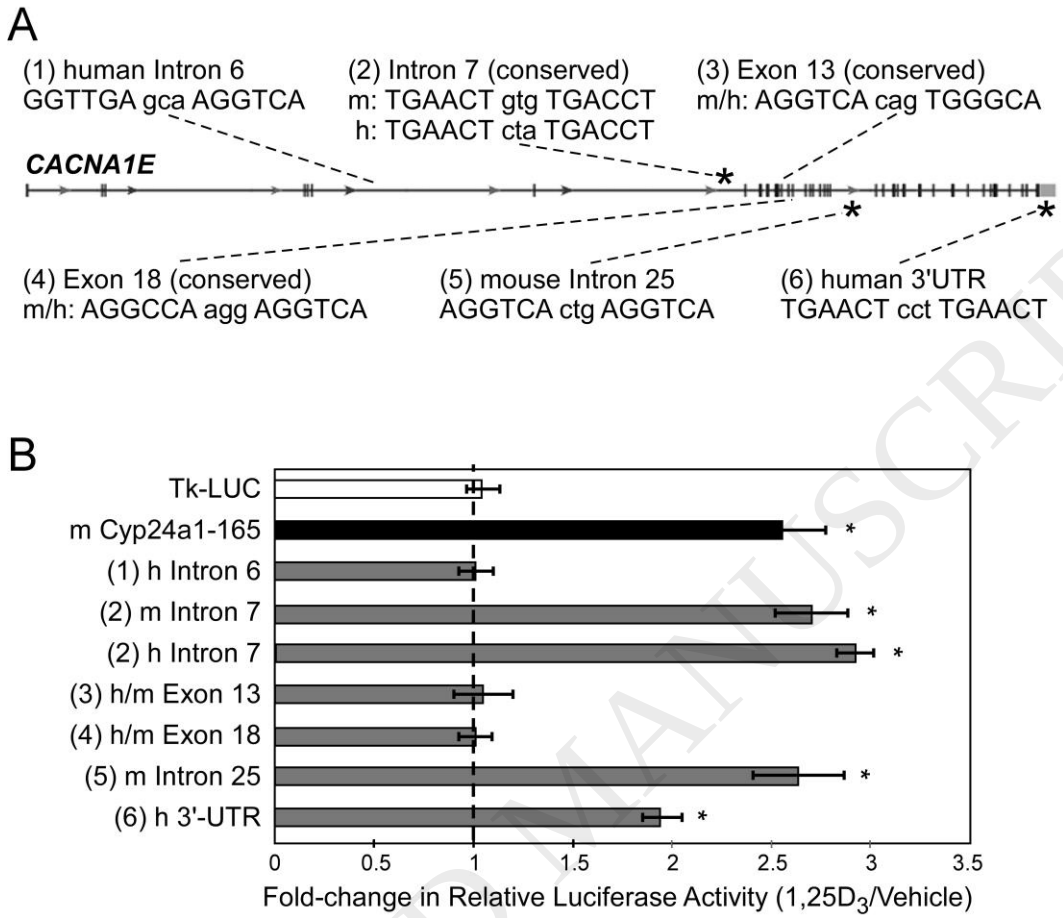

Fig. 6. The human and mouse Cav2.3 encoding genes contain conserved VDREs. **A**. *In silico* analysis of the *Cacna1e* genes was used to identify potential VDREs [26]. Four potential VDREs were found in the mouse *Cacna1e* gene and five potential VDREs were found in the human *CACNA1E* gene. The location and sequence of these VDREs is provided, and the VDREs denoted by asterisk showed VDR-dependent transactivation capacity by cell reporter assay. **B**. Cell reporter assays were performed in HEK293 cells. Cells were transfected with: reporter plasmids containing two copies of each VDRE upstream of the thymidine kinase minimal promoter and luciferase gene (the mouse CYP24a1-165 VDRE was used as a positive control); the expression plasmid, CMV-β-Galactosidase (to correct for transfection efficiency); and expression plasmids for the nuclear receptors (CMV-VDR and CMX-RXRα). Transfected cells were exposed to $1,25D_3$ or vehicle for 16 hours and then assayed for luciferase activity. $1,25D_3$-dependent changes in VDRE-mediated transcription are expressed as fold-change in relative luciferase activity (X-axis) for each VDRE (y-axis), and those VDRE facilitating a significant effect are denoted by asterisk ($p<0.05$). All data are shown as the mean ± S.E.M. ($n = 4$).

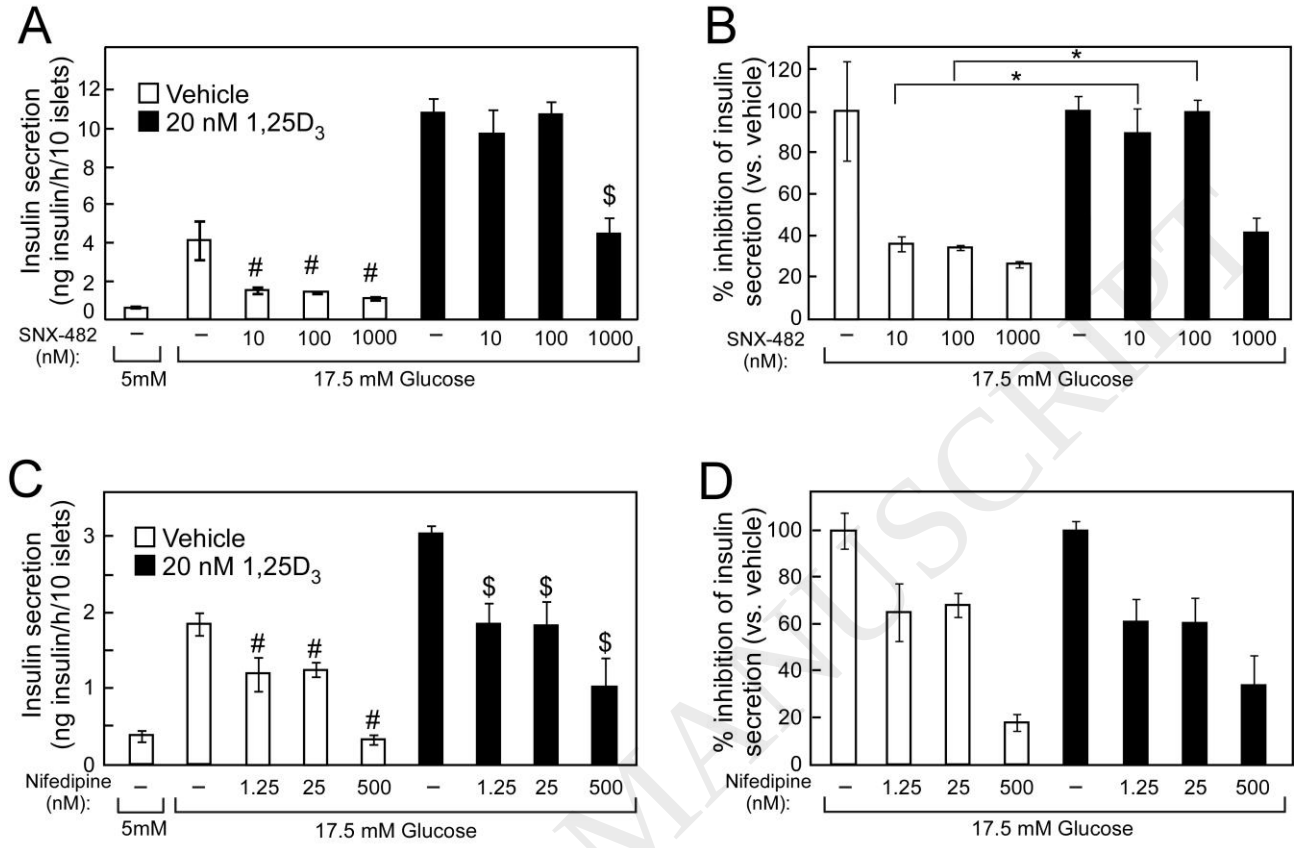

FIG. 7. Glucose stimulated insulin secretion suggests that 1,25D$_3$ upregulates a version of CaV2.3 that produces an R-type current that is resistant to chemical inhibition. Islets isolated from A129/Sv mice were incubated in vehicle (DMSO) or 20 nM 1,25D$_3$ for 16 hours, then transferred to secretion buffer (lacking glucose and 1,25D$_3$) for 1h, then transferred to secretion buffer supplemented with low glucose (5 mM) or high-glucose (17.5 mM) for insulin collection for 1h. The VGCC inhibitors, SNX-482 and nifedipine, were present both during the 1 hour incubation period prior to insulin collection and during the 1 hour GSIS period. **A**. SNX-482 dose-response effect on GSIS from islets pre-treated with vehicle or 1,25D$_3$. **B**. Data from A expressed as percent inhibition by SNX-482 on GSIS. **C**. Nifedipine dose-response effect on GSIS from islets pre-treated with vehicle or 1,25D$_3$. **D**. Data from C expressed at percent inhibition by Nifedipine on GSIS. All data are shown as the mean ± S.E.M. ($n \geq 4$), and were evaluated by ANOVA ($p<0.05$).